Computer simulation of molten silica and related glass forming fluids: recent progress

2007 J. Phys.: Condens. Matter 19 205102

(http://iopscience.iop.org/0953-8984/19/20/205102)

IOP PUBLISHING JOURNAL OF PHYSICS: CONDENSED MATTER

J. Phys.: Condens. Matter **19** (2007) 205102 (9pp) doi:10.1088/0953-8984/19/20/205102

Computer simulation of molten silica and related glass forming fluids: recent progress

K Binder, J Horbach, H Knoth and P Pfleiderer

Institut für Physik, Johannes Gutenberg-Universität Mainz, Staudinger Weg 7, 55099 Mainz, Germany

Received 2 October 2006
Published 25 April 2007
Online at stacks.iop.org/JPhysCM/19/205102

Abstract

The structure and dynamics of glass forming fluids are accessible in atomistic detail through molecular dynamics simulation. Although for molten silica and its mixtures with oxides of sodium, lithium, aluminium etc only systems at rather high temperatures can be fully equilibrated, since only timescales less than 100 ns are accessible, valuable insight can be gained, including guidance for corresponding experiments. A survey of the state of the art of such simulations and an outlook on open problems will be given.

(Some figures in this article are in colour only in the electronic version)

1. Introduction

Amorphous materials such as window glass have been produced for thousands of years, but nevertheless are poorly understood as regards their nanoscale structure [1–3]. In particular, the theoretical understanding of the slowing down of the undercooled fluid and the glass transition is a 'grand challenge problem' [1–4]. Also it has been debated what different classes of glass forming fluids exist. One popular distinction is based on the 'Angell plot' [5], where the logarithm of the shear viscosity $\eta(T)$ is plotted versus inverse temperature, normalized by the glass transition temperature, T_g/T (here T_g is determined ad hoc using the empirical rule $\eta(T = T_g) = 10^{13}$ P). Then 'strong glass formers' yield a straight line (i.e., an Arrhenius relation $\log \eta(T) \propto E_A/k_B T$ where E_A is some activation energy), while 'fragile glass formers' exhibit pronounced curvature (often $\eta(T)$ is described using a Vogel–Fulcher relation [1–3], $\log \eta(T) \propto E'_A/k_B(T - T_0)$, with the 'Vogel–Fulcher temperature' T_0 ($<T_g$) sometimes being associated with the 'Kauzmann temperature' [6]).

Molten silica (SiO_2) is the 'archetype' of a strong glass former [5]. Recent molecular dynamics simulations [7–16], using the BKS potential [17] have shown that this simple model provides a surprisingly good account for a wealth of experimental data. Moreover, these simulations (that we shall briefly recall in section 2) can 'go beyond experiment', i.e. be used to study the system at very high temperatures (2750–6100 K [8–11]) inaccessible to real

experiments, and it was found that at high temperatures the behaviour of $\eta(T)$ (and of the self-diffusion constants $D_O(T)$, $D_{Si}(T)$) resembles the behaviour of fragile glass formers. In fact, a rather compelling fit to the mode coupling theory (MCT) [4] of the glass transition could be made [12, 13, 16], yielding a MCT critical temperature $T_c \approx 3330$ K [12, 13]. While prior to this discovery the apparent lack of the existence of T_c for 'strong glass formers' called general concepts on the glass transition such as MCT [4] and the 'random first-order transition' scenario [3, 18–23] into question, it now appears that the distinction between strong and fragile glass formers is less fundamental than previously thought.

Of course, it is important to base such a conclusion on the study of more than a single material. In fact, related strong glass formers are mixtures of SiO_2 with various other oxides (Al_2O_3, Na_2O, K_2O, Li_2O, ...), and such multi-component silicate melts in fact are very important materials in the glass industry [24] and in the geosciences. In this paper we hence focus on the conclusions that can be drawn from our recent simulations on such mixed oxide melts [24–32], sections 3–5.

2. Molten and glassy silica studied using molecular dynamics

In molecular dynamics (MD) simulations averages are computed along the trajectories from Newton's equations of motion, using effective potentials for the interactions between the atoms [33]. Thus, quantum mechanical effects are neglected from the outset. It is perhaps a lucky accident that for SiO_2 a rather accurate description in terms of a simple pair potential [17] works. This so-called BKS potential is given by

$$\phi_{\alpha\beta}(r) = q_\alpha q_\beta e^2/r + A_{\alpha\beta}\exp[-B_{\alpha\beta}r] - C_{\alpha\beta}/r^6 \qquad \text{with } \alpha, \beta = \{\text{Si, O}\}. \tag{1}$$

Here, r is the distance between an ion of species α and another ion of species β, and e is the elementary charge while $q_{Si} = 2.4$ and $q_O = -1.2$ are chosen. The values for the parameters $A_{\alpha\beta}$, $B_{\alpha\beta}$ and $C_{\alpha\beta}$ of the Buckingham potential are found in [17]. This potential was derived using quantum chemistry methods [17] and describes both molten [7–15] and crystalline [34–37] SiO_2 rather well, although certain shortcomings on very small scales have been documented by comparison with '*ab initio* MD' methods [38, 39]. Due to the careful choice of parameters in equation (1), one effectively simulates the presence of directional covalent bonds through pair potentials.

In spite of the simplicity of the potential, its use for MD is nevertheless demanding in computer resources, since the long range of the Coulomb interaction requires the use of Ewald summation [33], and a very small time step ($\delta t = 1.6$ fs) is necessary to make integration errors negligible (as an integrator the 'velocity Verlet' algorithm is used [33]). Also, rather large simulation boxes (containing $N = 8016$ atoms) are needed to avoid finite size effects [8–15].

In fluid silica the structural relaxation time τ (which is proportional to $\eta(T)$) increases dramatically as the temperature is lowered. We fix the density of liquid SiO_2 at $\rho_{sim} = 2.37$ g cm^{-3} with this choice, the pressure is always positive in the temperature range under consideration. The latter value for the density exceeds the experimental density by about 10%, but this density difference leads only to minor changes of structural and dynamic properties in this case [7, 12]. The lowest temperature equilibrated by Horbach *et al* [8–13] was $T = 2750$ K, which is still far above the melting temperature. Cooling down from there to room temperature ($T = 300$ K) very fast (with a cooling rate of order 10^{12} K s^{-1}), glassy structures are produced [12] that agree very well with experiment, as far as we can tell from the comparison with the structure factor obtained [40] from neutron scattering. Also the temperature dependence of the specific heat [10] is in good agreement with corresponding experimental data, as well as the temperature dependence of longitudinal and transverse sound velocities [14].

Crucial for the above conclusion—that SiO_2 at high T is compatible with MCT and hence there is no fundamental difference between fragile glass formers and this strong glass former—is the behaviour of transport coefficients in the fluid phase, of course. For $10^4/T > 2.5\ \mathrm{K}^{-1}$ both D_{Si} and D_{O} follow Arrhenius laws with $E_{\mathrm{A}}^{\mathrm{O}} = 4.66$ eV, $E_{\mathrm{A}}^{\mathrm{Si}} = 5.18$ eV [8–10, 12]. These results agree with experimental data ($E_{\mathrm{A}}^{\mathrm{O}} = 4.7$ eV [41], $E_{\mathrm{A}}^{\mathrm{Si}} = 6$ eV [42]), even though the experiments were conducted at far lower temperatures. For $1.5\ \mathrm{K}^{-1} < 10^4/T < 2.5\ \mathrm{K}^{-1}$, on the other hand, the plots of $\ln D_\alpha$ versus $1/T$ exhibit strong curvature and can be well fitted to power laws ($D_\alpha \propto (1 - T_{\mathrm{c}}/T)^\gamma$ [12] with $T_{\mathrm{c}} = 3330$ K). The behaviour of the viscosity corroborates [12] these findings (although for $T > T_{\mathrm{c}}$ the Stokes–Einstein relation is violated).

But the key evidence in favour of MCT has been derived from a careful analysis of the dependence of the coherent and incoherent intermediate scattering functions $F(q,t)$, $F_{\mathrm{s}}(q,t)$ on wavenumber q and time t [8, 11–13]. One finds that these functions decay in two steps. For the first step ('β relaxation') a factorization property is predicted [4] to hold,

$$F(q,t) = F_{\mathrm{c}}(q) + h(q)G(t), \tag{2}$$

$F_{\mathrm{c}}(q)$ being the 'nonergodicity parameter' for the quantity considered and $h(q)$ some time-independent amplitude function, and $G(t)$ depends on time (and temperature, of course) only. This property can be directly tested by considering a function

$$R(t) = [F_{\mathrm{s}}(q,t) - F_{\mathrm{s}}(q,t')]/[F_{\mathrm{s}}(q,t'') - F_{\mathrm{s}}(q,t')], \tag{3}$$

if all times t, t', t'' lie in the β regime where equation (2) holds. Constructing $R(t)$ for various q all curves should superimpose in the β regime! Indeed one finds that this property holds already for one decade in time at $T = 4000$ K, while at lower temperatures it holds for two decades and more [11]. The nonergodicity parameter $F_{\mathrm{c}}(q)$ can be extracted from this analysis as well. On the other hand, using MCT it can be predicted from two- and three-particle correlators, i.e. purely from static input (also extracted from the simulation, however). Excellent agreement between MD simulations and this prediction is found [16]. We stress that no other theory exists that makes quantitative and testable predictions as MCT [4] does. Finally, we note that $F(q,t)$ and $F_{\mathrm{s}}(q,t)$ exhibit in the second relaxation step ('α relaxation') the well-known time–temperature superposition principle; and by fitting a law $\tau \propto (1 - T_{\mathrm{c}}/T)^{-\gamma}$ to the α relaxation time, one obtains another (and consistent) estimate for T_{c}.

3. Structure and transport properties in SiO_2–Al_2O_3 melts

Kramer *et al* [43] extended the BKS potential [17] to systems containing Na and Al, using effective charges $q_{\mathrm{Na}} = 1.0$, $q_{\mathrm{Al}} = 1.9$. Whereas for pure SiO_2 charge neutrality was maintained since $q_{\mathrm{Si}} = -2q_{\mathrm{O}}$, this is not the case for mixtures containing SiO_2 and Al_2O_3 (or also for mixtures of SiO_2 and Na_2O). Therefore for Na and Al ions the above potential was slightly modified, by introducing—somewhat ad hoc—distance-dependent charges $q_\alpha(r)$ for Na and Al that ensure charge neutrality [25–32]. We refer the reader to these papers for details on the potentials.

Figure 1 shows a comparison of the 'reduced' x-ray structure factor $q(S_{\mathrm{X}}(q) - 1)$ to experimental results [44, 45]. We note a rather good agreement.

However, the simulations can go beyond experiment and also record partial structure factors $S_{\alpha\beta}(q)$ or their combinations $S_{c_\alpha c_\alpha}(q)$ that are sensitive to concentration fluctuations. (If suitable different isotopes are available for the corresponding elements, these quantities are accessible to neutron scattering from samples with the same chemical composition but varying isotope content, but no suitable isotopes exist for Al.) In terms of the local concentration $c_\alpha(\vec{q})$ for particles of type α occurring at relative concentration $x_\alpha = N_\alpha/N$, where $N = \sum_\alpha N_\alpha$

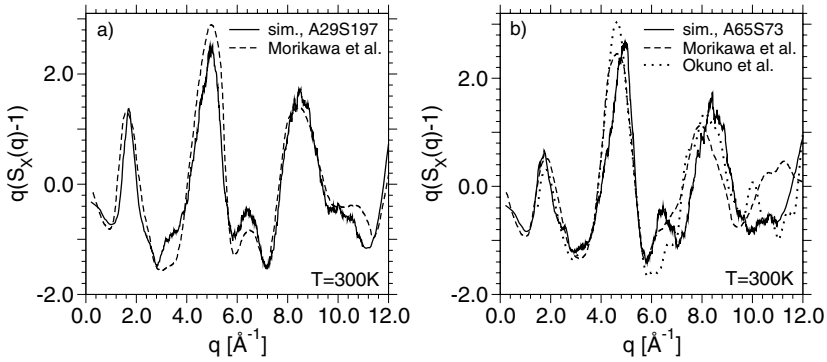

Figure 1. Reduced x-ray scattering factor $q(S_X(q) - 1)$ plotted versus q, as obtained from the MD simulation (full curves), compared to the available experimental data (dashed and dotted curves) [44, 45]. Part (a) refers to $29(Al_2O_3)$ $197(SiO_2)$, with about 13 mol% (Al_2O_3), from here on called A29S197; part (b) refers to $65(Al_2O_3)73(SiO)_2$, with about 47 mol% Al_2O_3, called A65S73. All data refer to $T = 300$ K. The simulated systems contain 2208 and 2176 atoms, respectively.

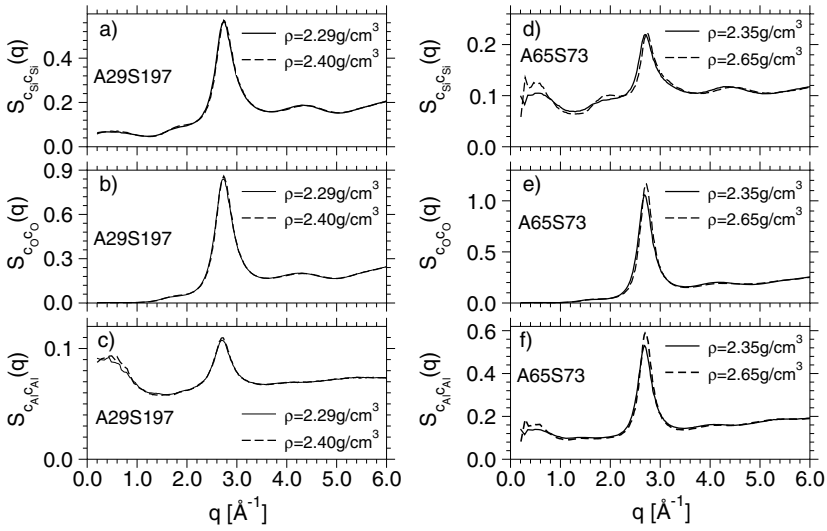

Figure 2. Structure factor $S_{c_\alpha c_\alpha}(q)$ for A29S197 ((a)–(c)) and for A65S73 ((d)–(f)) for α = Si ((a), (d)), O ((b), (e)) and Al ((c), (f)). Results are shown for different densities (as indicated). The temperature is $T = 2470$ K for A29S197. For A65S73, the temperatures are $T = 2100$ K and $T = 2000$ K for the low and the high density, respectively.

is the total number of all atoms, $c_\alpha(\vec{q}) = \rho_\alpha(\vec{q}) - x_\alpha \sum_\beta \rho_\beta(\vec{q})$, $\rho_\alpha(\vec{q}) = \sum_{k=1}^{N_\alpha} \exp(\mathrm{i}\vec{q} \cdot \vec{r}_k)$, where the sum extends only over particles of type α, one has [46]

$$S_{c_\alpha c_\beta}(\vec{q}) = \frac{1}{N} \langle c_\alpha(\vec{q}) c_\beta(\vec{q}) \rangle \tag{4}$$

Figure 2 shows three such structure factors, $S_{c_{Si}c_{Si}}(q)$, $S_{c_Oc_O}(q)$ and $S_{c_{Al}c_{Al}}(q)$, both for the model with 13 mol% Al_2O_3 and for the model with 47 mol% Al_2O_3. In $S_{c_{Al}c_{Al}}(q)$ (and to some extent also in $S_{c_{Si}c_{Si}}(q)$) one can clearly see a prepeak at about $q \approx 0.5$ Å^{-1}. Since $S_X(q)$, the x-ray structure factor, is dominated by $S_{c_Oc_O}(q)$ which does not show any signal

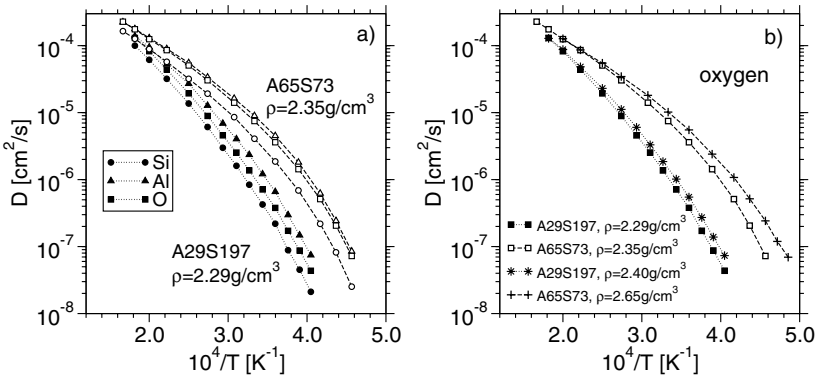

Figure 3. Arrhenius plots of the self-diffusion constants D_α, (a) for Si, Al and O for the different compositions at low densities, and (b) for oxygen for all systems considered as indicated.

of this prepeak, no prepeak can be detected in $S_X(q)$ either. The prepeak seen in these partial structure factors is indicative of microphase separation into a percolating network of Al-rich and Si-rich regions, while the oxygens remain homogeneously distributed. We use here the term microphase separation to indicate that the chemical ordering leads to structural correlations on intermediate length scales that go beyond the distance between nearest neighbours. These structural correlations can also be seen in simulation snapshots [32], and can be interpreted as a precursor effect of the (metastable) liquid–liquid phase separation below $T_{\rm crit} \approx 1900$ K that is found experimentally [47]. This phase separation is no surprise, since Al^{3+} ions need a different environment of O^{2-} ions to Si^{4+} ions. In SiO_2, each Si^{4+} ion (in the glass and supercooled fluid) is in the centre of a tetrahedron, with O^{2-} ions on the corners of the tetrahedron, and each O^{2-} ion is 'shared' by two neighbouring tetrahedra, and by these chemical rules an ideal continuous random network structure is created. However, fluid and amorphous Al_2O_3 samples have different structural units: threefold-coordinated oxygen atoms and fivefold- and sixfold-coordinated aluminium atoms. At low Al_2O_3 concentrations, one may encounter AlO_4 units in the network, but these are accompanied by so-called triclusters, i.e. structural units where an oxygen is surrounded by three cations, of which at least one is Al [30, 48]. It turns out that this disorder in the chemical structure of the networks makes the network less rigid than in the case of pure SiO_2, and enables a much faster self-diffusion [30, 32] than in the case of pure SiO_2. Figure 3 shows that over a wide range of inverse temperature the plot of $\log D$ versus $1/T$ exhibits curvature, for a wide range of concentrations. Interestingly, an anomalous behaviour of D_O with respect to pressure emerges: the diffusion becomes faster with increasing pressure. This probably can be attributed to the fact that more triclusters and fivefold-coordinated silicon atoms occur in the high density system, and by these defects in the ideal network structure diffusion is facilitated. Already in pure SiO_2 melts the presence of oxygen defects (fivefold- and threefold-coordinated Si atoms) is necessary to allow for oxygen diffusion [12]. Thus both increasing pressure and increasing content of Al_2O_3 in SiO_2 enhance the fragility of the system.

Again an analysis of intermediate scattering functions (see figure 4), as was done for pure SiO_2, reveals consistency with a MCT description [49].

4. Mixtures of silicon dioxide melts with alkali oxide melts

Simulations of fluid mixtures of SiO_2 with Na_2O at various compositions also revealed clear evidence of microphase separation [25–29]. This microphase separation can be attributed to

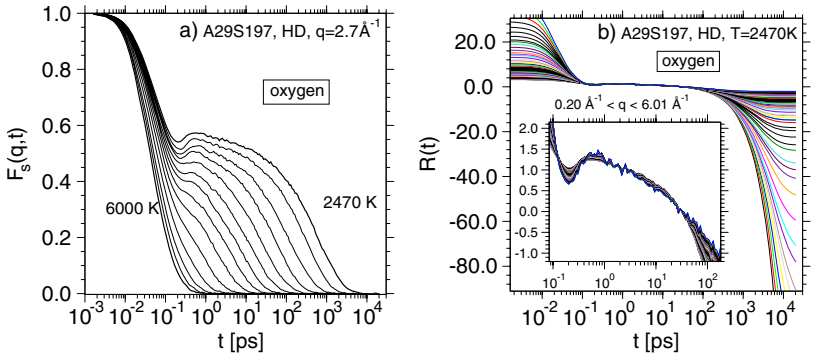

Figure 4. Intermediate scattering function $F_s(q, t)$ of the oxygen atoms plotted versus time for $q = 2.70$ Å^{-1} and 13 mol% Al_2O_3 at various temperatures from $T = 6000$ K down to $T = 2470$ K, from left to right (part (a)), and a test of the factorization property at $T = 2470$ K (part (b)).

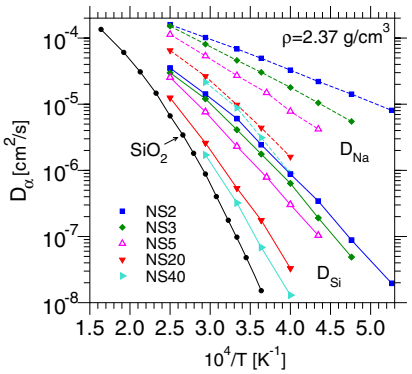

Figure 5. Arrhenius plot of the self-diffusion coefficients of Si and Na in SiO_2 and sodium silicate melts $(Na_2O)(xSiO_2)$ (denoted as NSx in the figure) with $x = 2$, 3, 5, 20 and 40.

the formation of Na-rich percolating channels, with a characteristic diameter of about 7 Å. This chemical inhomogeneity also shows up through a prepeak in the partial static structure factors, and in this case careful experiments could confirm its existence [50]. But unlike the microphase separation in the SiO_2–Al_2O_3-mixtures, where both Si and Al ions are tightly bound to the covalently bonded network, and hence all diffusion constants have similar magnitude (see figure 3), the sodium ions break the continuous random network up, creating dangling Si–O bonds. The Na atoms in the Na-rich channels, not being tightly bound to the SiO_2 network, have a much higher mobility (figure 5) [28] and so in this system one has both a static inhomogeneity on a mesoscopic length scale and a resulting inhomogeneity of the dynamic behaviour caused by this static inhomogeneity. This 'dynamic inhomogeneity' caused by microphase separation should not be confused with the 'dynamic heterogeneity' [51] well known for chemically homogeneous glass formers (such as one-component fluids). In any case it is remarkable that also for this system MCT is applicable and makes useful predictions [52]. The averaged equilibrium partial static structure factors suffice as input for explaining the fast sodium ion dynamics, at least qualitatively [52].

However, here we focus on another aspect of the dynamic inhomogeneity that arises if SiO_2 is mixed with two different alkali oxides: the 'mixed alkali effect' [53–56]. In such mixtures

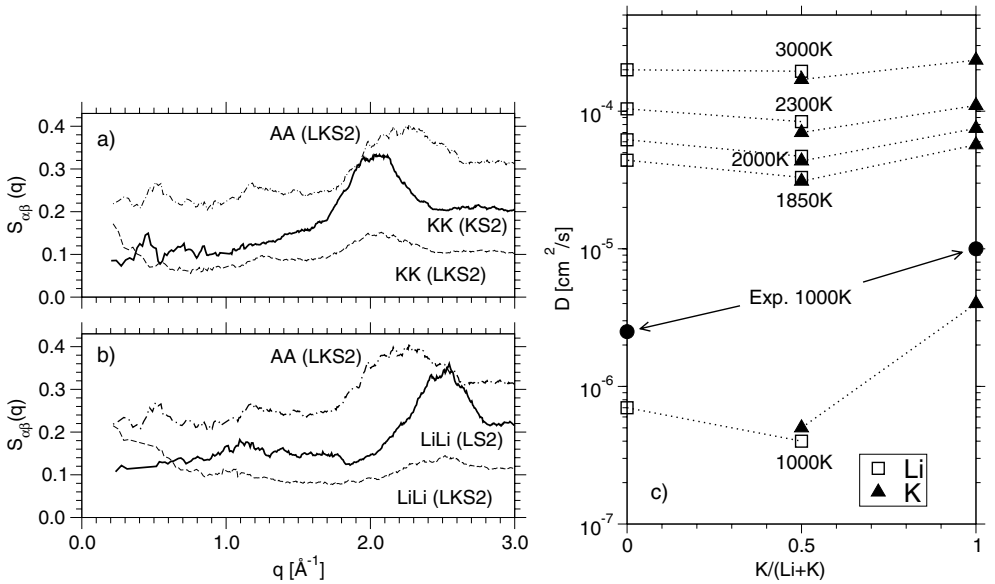

Figure 6. Partial structure factors $S_{\alpha\beta}(q)$ at $T = 1000$ K ((a), (b)). Part (a) shows $S_{\mathrm{KK}}(q)$ for KS2 and LKS2 and (b) $S_{\mathrm{LiLi}}(q)$ for LS2 and LKS2. Also included are $S_{\mathrm{AA}}(q)$ for LKS2 where A denotes an alkali ion without distinguishing between K and Li. Note that the curves of $S_{\mathrm{AA}}(q)$ are shifted upwards by 0.2. Part (c) shows the diffusion constants at the indicated temperatures as a function of x_{K}, which is the number of K ions with respect to the total number of alkali ions. The experimental data for $T = 1000$ K are taken from the literature.

with two alkali oxides the self-diffusion constants of the alkali ions may be orders of magnitude smaller than in the corresponding systems with only one alkali component.

We study this problem for the systems $(Li_2O)(2{\cdot}SiO_2)$ [LS2], $(K_2O)(2{\cdot}SiO_2)$ [KS2], and $(0.5{\cdot}Li_2O)(0.5{\cdot}K_2O)(2SiO_2)$ [LKS2], using the potential of Habasaki *et al* [57]. Carrying out simulations for 8064 atoms, again partial structure factors were obtained (figures 6(a), (b)). One finds prepeaks at around $q = 0.5$ Å^{-1} in $S_{\mathrm{KK}}(q)$ for KS2 and around 1.2 Å^{-1} in $S_{\mathrm{LiLi}}(q)$ for LS2 [31]. These prepeaks again can be interpreted as being due to formation of alkali-rich channels that percolate through the SiO_2 network, as for the SiO_2–Na_2O mixtures discussed above. Also included in figure 6 is the structure factor for the AA correlations in LKS2 where A denotes an alkali ion without distinguishing between Li and K. The latter function now exhibits prepeaks both around $q = 0.5$ and 1.2 Å^{-1}, i.e. at the same wavenumbers as the prepeak positions in the binary systems KS2 and LS2, respectively. This fact indicates that now there are two subnetworks of channels for each alkali species, characterized by somewhat different length scales. This conclusion is corroborated by a detailed analysis of simulation snapshots [31].

Figure 6(c) shows the self-diffusion constants for the different temperatures as a function of the potassium concentration $x_{\mathrm{K}} = N_{\mathrm{K}}/(N_{\mathrm{K}} + N_{\mathrm{Li}})$. For $T \geqslant 1850$ K only a very weak indication of a mixed alkali effect is seen, while for $T = 1000$ K one sees that D for $x_{\mathrm{K}} = 0.5$ is a factor of 3 smaller than D_{Li} for LS2 and a factor of 10 smaller than D_{K} for KS2. The reason for this behaviour is that the two alkali ion subnetworks in LKS2 are stiffer than the channel networks in LS2 and KS2; thus the alkali sites are more localized. It turns out to be very unlikely for a Li atom to hop to a site for a K atom in the K channel, or vice versa. The stronger binding of the alkali atoms in LKS2 to sites in their respective subnetwork is reflected in a higher activation energy in this system.

5. Discussion

In this paper, a comparative overview of molecular dynamics simulations of SiO_2 and its mixtures with Al_2O_3 and various alkali oxides is given. Simple pair potentials, such as the BKS potential [17], or variants thereof to include Na and Al ions [26, 30, 43], or the potential of Habasaki and Okada [57] that includes K and Li ions, were used. Comparison with various experimental results shows that these potentials allow for a rather reliable description of both structure and dynamics of these systems.

Although all these systems are prototype 'strong glass formers', the simulations show that mode coupling theory provides a good account for the initial stages of slowing down (at high temperatures, inaccessible to experiment, where the temperature variation of transport coefficients does not comply yet with the Arrhenius laws seen at lower temperatures). This finding is particularly remarkable in the oxide mixtures, since all of them have an inhomogeneous static structure at mesoscopic scales, which shows up in 'prepeaks' in certain partial static structure factors (which due to the lack of suitable isotopes are not accessible through neutron scattering experiments yet). In Al_2O_3–SiO_2 mixtures one finds microphase separation of Al and Si ions, associated with 'tricluster' formation near Al ions that cause 'chemical disorder' in the covalently bonded continuous random network structure. Here, all ions have very similar mobility. By contrast, in the mixtures of SiO_2 with alkali oxides the network is broken up, and channels rich in alkali ions form. The alkali ion diffusion is then characterized by much lower activation energies than either Si or O ion diffusion. However, if SiO_2 is mixed with two different alkali oxides, they form two separate channel networks, and not a common alkali channel network. Since the formations of two such percolating nets of different alkali ions within the covalently bonded SiO_2 net somewhat hinder each other, diffusion of alkali ions becomes much more difficult. Thus, our simulations confirm some basic ideas about the 'mixed alkali effect' and add atomistic insight into the detailed transport mechanisms in all these systems.

Acknowledgments

We thank W Kob, P Scheidler, K Vollmayr and A Winkler for their fruitful collaboration in stages of the work preceding the simulations presented here. Helpful discussions with W A Siebel are also acknowledged. Financial support came from the Emmy Noether Programme of the Deutsche Forschungsgemeinschaft (DFG), grant HO2231/2, and the Bundesministerium für Bildung und Forschung (BMBF), grant No 03N6015. We are grateful to the NIC Jülich and the HLRS Stuttgart for generous grants of computing time.

References

[1] Zallen R 1983 *The Physics of Amorphous Solids* (New York: Wiley)
[2] Jäckle J 1986 *Rep. Prog. Phys.* **49** 171
[3] Binder K and Kob W 2005 *Glassy Materials and Disordered Solids. An Introduction to Their Statistical Mechanics* (Singapore: World Scientific)
[4] Götze W and Sjögren L 1992 *Rep. Prog. Phys.* **55** 241
[5] Angell C A and Sichina W 1976 *Ann. New York Acad. Sci.* **279** 53
[6] Kauzmann W 1948 *Chem. Rev.* **43** 219
[7] Vollmayr K, Kob W and Binder K 1996 *Phys. Rev.* B **54** 15808
[8] Horbach J, Kob W and Binder K 1998 *Phil. Mag.* B **77** 297
[9] Horbach J and Kob W 1998 *J. Non-Cryst. Solids* **235–237** 320
[10] Horbach J, Kob W and Binder K 1999 *J. Phys. Chem.* B **103** 4104

[11] Kob W, Horbach J and Binder K 1999 *AIP Conf. Proc.* **469** 441
[12] Horbach J and Kob W 1999 *Phys. Rev.* B **60** 3169
[13] Horbach J and Kob W 2001 *Phys. Rev.* E **64** 041503
[14] Horbach J, Kob W and Binder K 2001 *Eur. Phys. J.* B **19** 531
[15] Scheidler P, Kob W, Latz A, Horbach J and Binder K 2001 *Phys. Rev.* B **63** 104204
[16] Sciortino F and Kob W 2001 *Phys. Rev. Lett.* **86** 327
[17] van Beest B H W, Kramer G J and van Santen R A 1990 *Phys. Rev. Lett.* **64** 1995
[18] Kirkpatrick T R and Thirumalai D 1988 *Phys. Rev.* B **37** 5342
[19] Mezard M and Parisi G 1996 *J. Phys. A: Math. Gen.* **29** 6515
[20] Mezard M and Parisi G 1999 *J. Chem. Phys.* **111** 1076
[21] Mezard M and Parisi G 2000 *J. Phys.: Condens. Matter* **12** 6655
[22] Parisi G 2000 *Physica* A **280** 115
Mezard M 2002 *Physica* A **306** 25
[23] Eastwood M P and Wolynes P G 2002 *Europhys. Lett.* **60** 587
[24] Fotheringham U, Binder K, Kob W and Horbach J 2005 *Glass Sci. Technol.* **78** 203
[25] Horbach J and Kob W 1999 *Phil. Mag.* B **79** 1981
[26] Horbach J, Kob W and Binder K 2001 *Chem. Geol.* **174** 87
[27] Horbach J, Kob W and Binder K 2002 *Phys. Rev. Lett.* **88** 125502
[28] Binder K, Horbach J, Kob W and Winkler A 2003 *Comput. Sci. Eng.* **5** 60
[29] Horbach J, Winkler A, Kob W and Binder K 2003 *Mater. Res. Symp. Proc.* **754** 147
[30] Winkler A, Horbach J, Kob W and Binder K 2004 *J. Chem. Phys.* **120** 384
[31] Knoth H, Horbach J and Binder K 2004 *Computational Modeling and Simulation of Materials* vol III, Part B ed P Vincenzini and A Lami (Firenze: Techna Group) p 3
[32] Pfleiderer P, Horbach J and Binder K 2006 *Chem. Geol.* **229** 186
[33] Binder K and Ciccotti G (ed) 1996 *Monte Carlo and Molecular Dynamics of Condensed Matter* (Bologna: Societa Italiana di Fisica)
[34] Tse J S and Klug D D 1991 *J. Chem. Phys.* **95** 9176
[35] Tse J S, Klug D D and Le Page Y 1992 *Phys. Rev.* B **46** 5993
[36] Müser M H 2001 *J. Chem. Phys.* **114** 6364
[37] Müser M H and Binder K 2001 *Phys. Chem. Miner.* **28** 746
[38] Benoit M, Ispas S, Jund P and Jullien R 2000 *Eur. Phys. J.* B **13** 631
[39] Benoit M and Kob W 2002 *Europhys. Lett.* **60** 269
[40] Price D L and Carpenter J M 1987 *J. Non-Cryst. Solids* **92** 153
[41] Mikkelsen J C 1984 *Appl. Phys. Lett.* **45** 1187
[42] Brébec G, Seguin R, Sella C, Bevenut J and Martin J C 1976 *Acta Metall.* **28** 327
[43] Kramer G J, de Man A J M and van Santen R A 1991 *J. Am. Chem. Soc.* **64** 6435
[44] Morikawa H, Miwa S, Miyake M, Marumo F and Sata T 1982 *J. Am. Ceram. Soc.* **65** 6435
[45] Okuno M, Zotov N, Schmücker M and Schneider H 2005 *J. Non-Cryst. Solids* **351** 1032
[46] Blétry J 1976 *Z. Naturf.* **319** 960
[47] MacDowell J F and Beall G H 1969 *J. Am. Ceram. Soc.* **52** 17
[48] Tossell J A and Horbach J 2005 *J. Phys. Chem.* B **109** 1794
[49] Pfleiderer P 2005 *Master Thesis* University of Stuttgart, unpublished
[50] Meyer A, Horbach J, Kob W, Kargl F and Schober H 2004 *Phys. Rev. Lett.* **93** 027801
[51] Sillescu H 1999 *J. Non-Cryst. Solids* **243** 81
Ediger M D 2000 *Ann. Rev. Phys. Chem.* **51** 99
Richert R 2002 *J. Phys.: Condens. Matter* **24** R703
[52] Voigtmann Th and Horbach J 2006 *Europhys. Lett.* **74** 459
[53] Day D E 1976 *J. Non-Cryst. Solids* **21** 343
[54] Ingram M D 1987 *Phys. Chem. Glasses* **28** 215
[55] Ingram M D 1999 *J. Non-Cryst. Solids* **255** 35
[56] Green P F (ed) 1999 *Selected Papers from the Symp. on Characterization of the Mixed Alkali Effect in Glasses*; *J. Non-Cryst. Solids* **255** special issue
[57] Habasaki J and Okada I 1992 *Mol. Simul.* **9** 319